Integrated Magneto Drive Unit with Synchronous Reluctance Motor

Saira Tariq
Département de génie électrique
École de technologie supérieure
Montreal, Canada
saira.tariq.1@ens.etsmtl.ca

Qingsong Wang
Département de génie électrique
École de technologie supérieure
Montreal, Canada
qinsong.wang@etsmtl.ca

Ambrish Chandra
Département de génie électrique
École de technologie supérieure
Montreal, Canada
ambrish.chandra@etsmtl.ca

Zhaoheng Liu
Département de génie mécanique
École de technologie supérieure
Montreal, Canada
zhaoheng.liu@etsmtl.ca

***Abstract*—The global transition toward electrified transportation and energy efficient industrial drives is intensifying the demand for electric machines. This paper proposes the design of a novel axially integrated magneto drive unit (IMDU) with synchronous reluctance motor. The structure and operating principle of the proposed machine is analyzed. Genetic optimization is used to globally optimize the design parameters of both the reluctance motor and the magnetic gear. Then the electromagnetic performance of the proposed IMDU is investigated using finite element analysis. Comparative studies between the proposed IMDU and conventional surface mounted permanent magnet machine has been conducted, and the results show that the average torque of the IMDU is 70.62% higher than surface permanent magnet machine with the same size, the same amount of magnet and the same current density.**

***Index Terms*—Genetic optimization, integrated magneto drive unit, magnetic gear, synchronous reluctance motor**

I. Introduction

In recent decades, there has been a significant focus on addressing energy crises and environmental pollution. The global consensus for the 21st century is to prioritize energy conservation and reduce emissions. Electrification has emerged as an alternative solution, particularly in various industrial applications, with a strong emphasis on the automotive sector. Thanks to rapid advancements in high-performance electric motors and power electronics technology, electric and hybrid electric vehicles (EV/HEVs) have been under investigation and development as potential replacements for traditional oil-fueled cars. Currently, commercially available battery electric and hybrid vehicles are gaining widespread acceptance worldwide. The global transition toward electrified transportation and energy efficient industrial drives is intensifying the demand for electric machines that combine high torque density, wide speed range, and reliable operation without relying on scarce or expensive materials. Conventional motor technologies have made substantial progress, yet they still face inherent trade-offs: permanent magnet motors offer high torque but depend on rare-earth elements [1], while reluctance motors avoid magnets but struggle to match the same torque output. In order to meet the requirements of high torque applications, a gearbox is usually used to amplify the torque generated by the electric motor. And many integrated designs [2] have been developed to reduce the size and increase power density. However, mechanical gearbox replies on the meshing of the teeth between the input and output rotors, which generates friction, reduces reliability and needs regular maintenance. Despite the advantages of mechanical gears, the transmission often suffers from problems associated with mechanical contacts, such as gear noise and vibrations, mechanical wear, as well as the need for lubrication, reduce the overall transmission system efficiency. Magnetic gear (MG) could be a good alternative of mechanical gear, which transmits torque through magnetic field and has no mechanical contact between the input and output rotors, and therefore, is more efficient and reliable [3-5]. The integration of magnetic gears and electrical machines has been widely investigated, and many magnetic-geared machines, also known as flux-modulated machines, have been proposed [6-9]. Although these machines could achieve a high torque density due to the gearing effect, they rely on salient pole structure to achieve flux modulation, which increases leakage flux, reduces power factor and increases noise and vibration. This paper introduces a novel integrated magneto drive unit (IMDU) that uniquely merges a synchronous reluctance motor (SynRM) with a coaxial magnetic gear into a single electromagnetic system, eliminating mechanical couplings and reducing axial length compared to conventional cascaded configurations. This paper proposed axially integration of SynRM and a magnetic gear into the same enclosure. Compared with traditional surface permanent magnet machines, the proposed IMDU achieves a higher torque density with the same volume of permanent magnets. Section II describes the structure and operating principle of proposed IMDU. Section III outlines the optimization of both the synchronous machine and the magnetic gear. In Section IV the electromagnetic performances of the optimized SynRM and MG are analyzed and compared

979-8-3315-8138-1

through 2D-FEA. Section V presents the comparative study between the proposed IMDU and traditional SPM. Finally, the conclusions are summarized in Section VI.

II. STRUCTURE OF THE PROPOSED IMDU

Fig. 1 shows the sectional view of the proposed IMDU and the exploded view is given in Fig. 2. The proposed IMDU axially integrates a SynRM and a MG in the same housing, to achieve a compact structure. The rotor of SynRM is connected to the inner rotor of MG through a common shaft, to allow the SynRM torque been amplified directly by the MG. The MG consists of two rotors and a modulator. The stator of the motor has the same diameter as the outer rotor of the MG and they are fixed to the housing and connected to each other using rods. The number of pole-pairs in the system can be determined from the space harmonic flux density distribution produced by either high or low speed rotor permanent magnets, is given by:

$$P_{m,k} = |m_p + kn_s|$$
$$m=1,3,5,\ldots,\infty$$
$$k=0,\pm1,\pm2,\pm3,\ldots,\infty$$

where p is the pole pairs number, and n_s is the number of ferromagnetic pole pieces.

Permanent magnets are surface mounted on the inner and outer rotors of the MG, and a modulation ring is sandwiched between the two rotors to achieve flux modulation and allow effective coupling between the magnetic fields generated by the inner and outer rotors. The design specifications of proposed IMDU are shown in Table I.

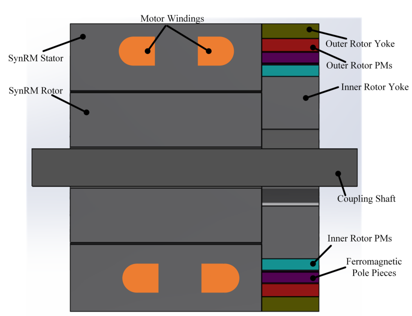

Fig. 1: Sectional view of the proposed IMDU.

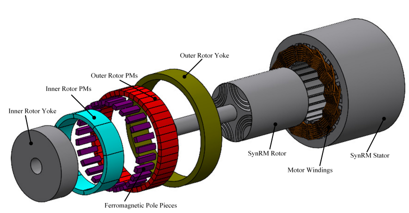

Fig. 2: Exploded view of the proposed IMDU.

III. MULTIOBJECTIVE GENETIC OPTIMIZATION

The initial design stage is always required to determine a good starting point in finding an optimum solution for the specific requirements of the design. However, in order to achieve maximum performance of the machine, the multi-objective optimization process is essential. Therefore, multi-variable optimization is implemented on the MG and SynRM to improve average torque and reduce torque ripple. Fig. 3 shows the flowchart of Genetic Optimization (GO).

TABLE I: DESIGN SPECIFICATIONS OF PROPOSED IMDU-SYNRM

	Design Parameters	Value
SynRM	Number of poles	4
	Number of stator slots	24
	Stack length	100mm
	Stator outer diameter	150mm
	Rotor outer diameter	78mm
	Operating Current	50A
	Air gap length	1mm
	Operating Speed	1000rpm
	Number of turns	18
	Material of Rotor and Stator	50A1000
MG	Number of pole pairs on high-speed rotor	4
	Number of pole pairs on low-speed rotor	22
	Number of ferromagnetic pole pieces	26
	Outer rotor outer diameter	150mm
	Inner rotor outer diameter	108mm
	Stack length	30mm
	Air gap b/w inner rotor and pole pieces	1mm
	Air gap b/w pole pieces and outer rotor	0.5mm
	Material of MG' pole pieces inner and outer yoke	50H470
	Material of MG' inner and outer rotor	NdFeB

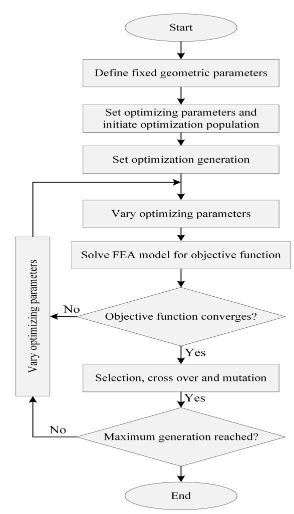

Fig. 3: Genetic optimization' execution steps.

The proposed multi-objective genetic optimization is formulated as below;

A. For MG

The studied problem is defined as follows:

979-8-3315-8138-1

$$\begin{cases} Obj1 : maxT_{avg} \\ Obj2 : minT_{ripp} \\ Obj3 : minvol_{PM} \\ Cons1 : B_{inner} \geq 0.5 \\ Cons2 : B_{outer} \geq 0.5 \end{cases}$$

The cross-sectional parameters are shown in Fig. 4(a). As can be seen there are 3 variables located on the MG design. Table II shows the variation range for the optimization parameters. The variation range has been selected in a manner that prevents possible geometrical errors during the optimization process. Moreover, due to proper initial design, the optimization process will have a faster convergence to the optimal designs.

TABLE II: DESIGN PARAMETERS RANGE FOR IMDU

Design parameters	Parameter	Range	Optimized
Inner Radius of Yoke	Rad_Yi (mm)	66-68	67.21
Pole Piece Angle	Ang_Pp (Mech.Deg)	2-13	7.31
Length of Pole Pieces	L_Pp (mm)	2.5-7.5	5.59

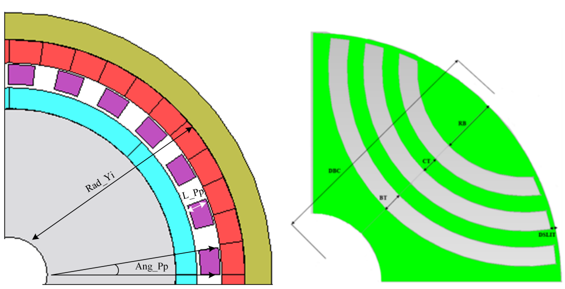

(a) (b)

Fig. 4: The parametric geometry for optimization purposes

B. For SynRM

For SynRM the objective functions of multiobjective genetic optimization are as under:

$$\begin{cases} Obj1 : maxT_{avg} \\ Obj2 : minT_{ripp} \end{cases}$$

The cross-sectional parameters are shown in Fig. 4(b). As can be seen there are 5 variables located on the SynRM design. Table III shows the variation range of design parameters for optimization for SynRM.

TABLE III: DESIGN PARAMETERS RANGE FOR SynRM

Design parameters	Parameter	Range	Optimized
Barrier Thickness	BT (mm)	1.943.25	3.25
Core Thickness	CT (mm)	1.573	3
Distance of Barrier Center	DBC (mm)	4548	48
Depth of slit	DSLIT (mm)	0.61.2	0.6
Radius of Barrier	RB (mm)	12-16.91	16.45

During the genetic optimization, the 2500 cases simulated. The number 2,500 cases are likely the product of Population Size (N)×Number of Generations (G). In this paper, it is used a population of 50 and ran it for 50 generations, 50 individuals are enough to cover the diverse variables of both a Magnetic Gear and a SynRM. The Genetic multiobjective optimization was performed on Dell-PC 64-bit operating system, x64- based processor with 8GB RAM, Intel (R) Xeon (R) w5-3435X CPU running at 3.10 GHz and took 27 hours; it occupied 23GBs space on the drive. The optimized average torque (T_{avg}) and the optimized torque ripples (T_{ripp}) with respect to various geometry variables are shown in Fig. 5.

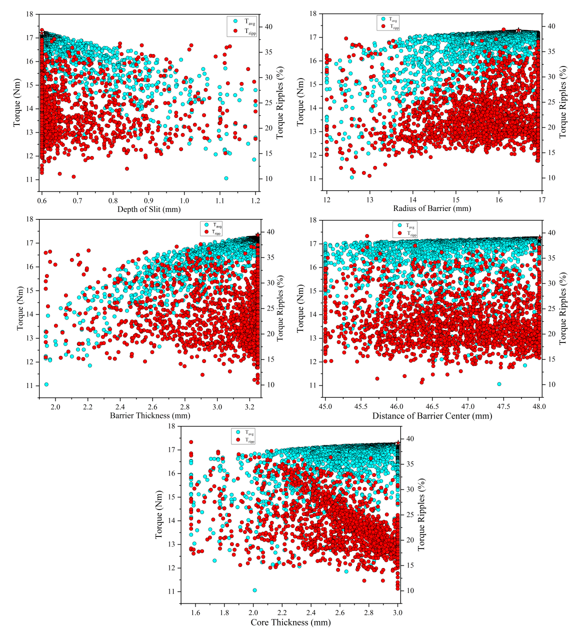

Fig. 5: Effect of optimization variables

IV. ELECTROMAGNETIC PERFORMANCE ANALYSIS

A. MG

The MG uses rare-earth PMs for both its inner rotor and outer rotor, as well as ferromagnetic pole pieces between its two rotors. All of these PMs play a significant role in transmitting torque. In fact, simulation studies have indicated that a gear of this kind could have a transmitted torque density capacity comparable to that of two- or three-stage helical gearboxes. As a result, when coupled with a conventional topology of SynRM, this magnetic gear could prove to be beneficial in applications as varied as embedded motor/generator sets.

To clearly exhibit the modulation effect in the MG, the waveforms of the radial flux density distribution in the inner and outer airgaps before and after the genetic optimization are demonstrated in Fig. 6. Fig. 7 (a) illustrate the variation in maximum torque on the low-speed rotor as a function of the radial thickness of the stationary pole-pieces, while keeping a constant airgap diameter side by side with the low-speed rotor and fixed amount of magnet material on both the low-speed

979-8-3315-8138-1

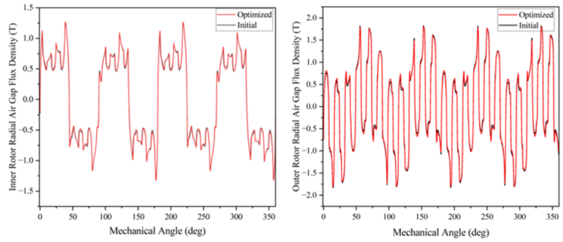

(a) (b)

Fig. 6: Radial flux density distribution (a) Inner rotor (b) Outer rotor.

and high-speed rotors. The results indicate the presence of an optimal pole-piece radial thickness that yields the highest torque transmission. Initially the output torque of the MG was 89.62 Nm. After genetic optimization, the output torque improved to 91.28 Nm. Although, in the above results, it has been demonstrated how the main parameters of MG design impact the average torque transmission, it is also necessary to consider the impact of torque ripples in the rotors, which may have a negative impact on performance. This torque ripple is also known as cogging torque. It is caused by the interaction between the rotor permanent magnets and the ferromagnetic pole pieces. In the optimized design, the inner rotor T_{ripp} are reduced by 30% and in the outer rotor T_{ripp} are reduced by 4.38% as shown in Fig. 7 (b). Table IV shows the performance comparison after genetic optimization.

TABLE IV: COMPARISON OF PERFORMCE OF CMG AFTER GO

Parameter	Initial	Optimized	Improvement
T_{out}	89.62 Nm	91.28 Nm	1.85%
T_{in}	16.26 Nm	16.34 Nm	0.49%
Inner $T - ripp$	4.0%	2.8%	30%
Outer T_{ripp}	0.52%	0.31%	4.38%
Inner B_r	-5.167e-6	5.807e-6	212.39%
Outer B_r	2.039e-5	1.858e-5	8.88%

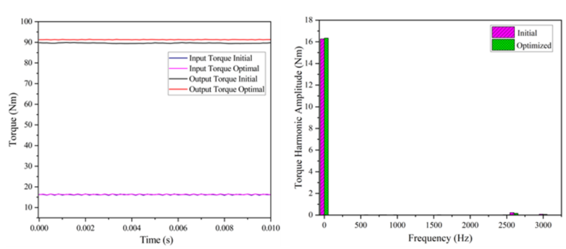

(a) (b)

Fig. 7: (a) Output Torque on low-speed rotor, (b) Torque Harmonic Amplitude of MG

B. SynRM

A better electric machine performance can arise due to a stronger magnetic field, which specifies a higher air-gap magnetic flux density. The radial magnetic flux density before and after the genetic optimization is shown in Fig. 8 (a). Also Fig. 8 (b) shows the measured radial flux in the air gap along with the harmonic spectra. Fig. 9 shows the magnetic flux density distribution for the proposed SynRM.

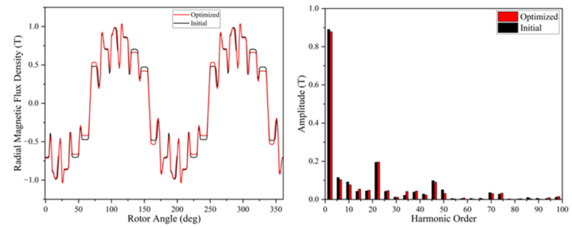

(a) (b)

Fig. 8: Radial flux density wave form along with harmonic spectra

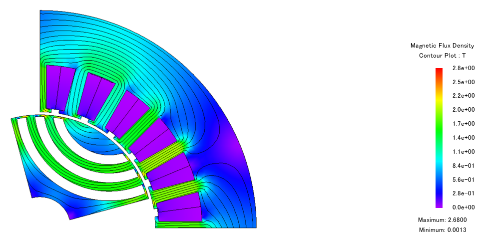

Fig. 9: Flux density distribution in the SynRM

The two important characteristics in machine design are Torque/Ampere capability and efficiency. In the SynRM torque is expressed by:

$$T = (3/2)(p/2)(L_d - L_q).i_d i_q = (3/2)(p/2)(L_d - L_q).I_s^2.sin(2\theta) \quad (1)$$

Where p is pole number, I_s is the stator rms current, and θ is the current angle. During multi objective genetic optimization, the main objective is average torque enhancement. Initially, the average torque of the presented SynRM was 16.55Nm. After the genetic optimization, the average torque improved to 17.35Nm, which is 4.85% greater than the initial design as shown in Fig. 10.

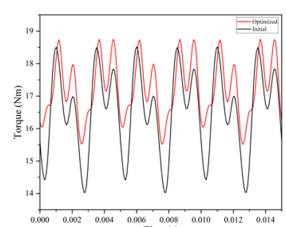

Fig. 10: Average torque in proposed SynRM.

The 3D view of the SynRM is showed in Fig. 11. It also shows the comparison between initial and optimized torque. Table V shows the comparison of performance of SynRM after GO.

979-8-3315-8138-1

TABLE V: PERFORMCE COMPARISON OF SynRM AFTER GO

Parameter	Initial	Optimized	Improvement
T_{avg}	16.55 Nm	17.35 Nm	4.85%
T_{ripp}	27.10%	18.78%	30.70%
3D T_{avg}	16.45 Nm	17.20 Nm	4.56%
B_r	-6.17e^{-18}	1.05e^{-16}	1801.7%

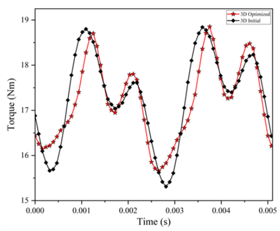

Fig. 11: 3D Torque for SynRM.

C. IMDU

By combining both the magnetic gear and electric machine, the system efficiency and power density are further improved. The system structure will also be more compact and lighter, reducing costs associated with lubrication and maintenance. It's very useful for different applications, such as e-mobility and electricity production. As shown in Fig. 12, the average torque of SynRM is significantly enhanced by IMDU.

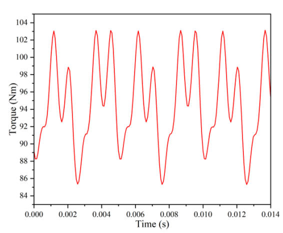

Fig. 12: Average torque of proposed IMDU.

V. PERFORMANCE COMPARISON WITH SURFACE MOUNTED PERMANENT MAGNET SYCHRONOUS MACHINE

The SynRM shows significantly lower performance than Permanent Magnetic Synchronous Machine (PMSM). Even if the rotor design is changed somewhat, this will probably only result in small changes. In either way, the T_{avg} is not sufficient enough to replace PMSM. One interesting aspect that needs to be considered is enhanced average torque after integration of MG. By running 2D FEA with same current density, operating current, rated speed, PM volume, stack length, it can be seen in Fig. 13 that proposed IMDU has 70.62% higher T_{avg} than SMPMSM.

VI. CONCLUSION

The Integrated Magneto Drive Unit (IMDU) combined with a synchronous reluctance motor has been presented in this paper. The proposed structure and operating principles were

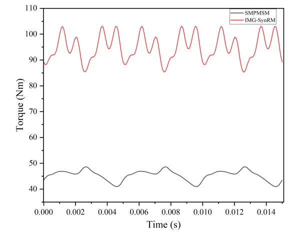

Fig. 13: Comparison of average Torque between SMPMSM and IMDU.

rigorously analyzed, genetic optimization algorithm is used to improve and optimize the design specifications globally. Comprehensive FEA confirmed the electromagnetic performance of the proposed design. The performance comparison between the conventional SMPMSM and the proposed design of IMDU shows the supremacy of the proposed design over the presented design in the literature. In conclusion, when compared with the conventional SMPMSM, the proposed IMDU possesses 70.62% higher average torque than a conventional SMPMSM of equivalent size, magnetic material volume, and current density. This highly significant finding establishes the IMDU as a compelling, high-torque-density solution that is well-suited to meet the escalating performance and efficiency demands of future electrified transportation and industrial drive applications.

REFERENCES

[1] I. Boldea, F. Marignetti, G. Graber, M. Porzio and L. Fratelli, "PM-free electric motor powertrains in road and rail transport: an overview," IEEE International Conference on Electrical Systems for Aircraft, Railway, Ship Propulsion and Road Vehicles & International Transportation Electrification Conference (ESARS-ITEC), pp. 1-9, 2023.

[2] G. Cooke, R. -S. Dragan, R. Barrett, D. J. Powell, S. Graham and K. Atallah, "Magnetically Geared Propulsion Motor for Subsea Remote Operated Vehicle," IEEE Transactions on Magnetics, vol. 58, no. 2, pp. 1-5, 2022.

[3] D. Fodorean, 'State of the Art of Magnetic Gears, their Design, and Characteristics with Respect to EV Application', Modeling and Simulation for Electric Vehicle Applications. InTech, Oct. 05, 2016.

[4] Ruiz-Ponce, G., Arjona, M. A., Hernandez, C., & Escarela-Perez, R. (2023). A Review of Magnetic Gear Technologies Used in Mechanical Power Transmission. Energies, 16(4), 1721.

[5] K. Atallah and D. Howe, "A novel high-performance magnetic gear," IEEE Trans. Magn., vol. 37, no. 4, pp. 2844–2846, 2001.

[6] K. T. Chau, Electric Vehicle Machines and Drives – Design Analysis and Application., Hoboken, NJ, USA:Wiley-IEEE Press, 2015.

[7] L. Jing, W. Tang, T. Wang, T. Ben and R. Qu, "Performance Analysis of Magnetically Geared Permanent Magnet Brushless Motor for Hybrid Electric Vehicles," in IEEE Transactions on Transportation Electrification, vol. 8, no. 2, pp. 2874-2883, 2022.

[8] X. Zhu, CHT Lee, C. C. Chan, L. Xu, and W. Zhao, "Overview of flux-modulation machines based on flux-modulation principle: Topology, theory, and development prospects," IEEE Transactions on Transportation Electrification, vol. 6, no. 2, pp. 612-624, 2020.

[9] B. Ion, L. N. Tutelea, and A. Popa, "Reluctance synchronous and flux-modulation machines designs: Recent progress," IEEE Journal of Emerging and Selected Topics in Power Electronics, vol. 10, no. 2, pp. 1683-1702, 2021.

979-8-3315-8138-1